Part II. Experimental Studies

A horizontal, rectangular channel of high aspect ratio has been built for the study of interphase mass transfer in stratified, laminar gas-liquid flow. Cases were examined where the resistance to mass transfer is confined to the gas phase and where the control is distributed between phases. Measurements of the rate of evaporation of ethanol into oxygen and carbon dioxide confirmed that cocurrent interface motion enhances gas phase-controlled mass transfer coefficients substantially. On the other hand countercurrent motion of the interface decreases the coefficient. Agreement with basic convective diffusion theory was found for the evaporation of ethyl ether into helium and carbon dioxide from dilute solutions in ethanol, cases where the mass transfer control is distributed between the phases. Experiments with aqueous solutions were hampered by the accumulation of surfactants at the interface. A diaphragm cell technique was used to measure diffusivities of 0.87 $\times$ 10^{-5} sq.cm./sec. for ethyl ether at high dilution in ethanol and 0.96 $\times$ 10^{-5} sq.cm./sec. for ethyl ether at high dilution in water at 25°C.

Industrial gas-liquid contacting operations, such as absorption and distillation, often involve chemical systems where the resistance to mass transfer is distributed between phases. In addition the fluid mechanics of the two contacting phases are normally such that the liquid interface is in either cocurrent or countercurrent motion relative to the gas stream. In many situations there is substantial heat transfer occurring simultaneously with mass transfer. Sufficiently high flux rates of heat and mass transfer can give rise to interfacial instabilities, such as Bénard cells and Marangoni effects. The complexity of industrial equipment makes it unacceptable for laboratory studies of the underlying processes. Therefore laboratory models have been developed for study of the important problems involved in interphase mass transfer. Such devices as wetted-wall columns and laminar liquid jets have been used to investigate interphase mass transfer under relatively simple flow conditions.

These experiments have almost always involved situations where one of the phases presents a controlling resistance to mass transfer. There are two basic reasons for this preponderance of studies with single-phase control. First, the design of most devices is such that the fluid mechanics of only one phase are simple. To analyze the behavior of the other phase it is usually necessary to resort to some empiricism. A good example of this is the laminar jet. Scriven and Pigford (*18, 19*) used a jet to measure the absorption of carbon dioxide into water, a liquid phase-controlled process. Their data are successfully correlated by the use of a modified penetration theory. Several years later Hatch and Pigford (*10*) altered the apparatus to allow continuous flow of the gas phase and measured rates of absorption of ammonia into water, a strongly gas phase-controlled process. The fluid mechanics in the gas phase were found to be quite complex, and dimensional analysis was required to correlate the data.

The second reason for the large number of studies with single-phase control lies in the fact that in 1922 and 1923 Lewis (*15*) and Whitman (*24*) developed their two-film theory for interphase mass transfer. They postulated that the resistance to mass transfer is confined to two thin films near the interface and therefore the individually measured resistances to mass transfer could be added. If this principle were universally valid, the need to study mass transfer with the resistance distributed between the phases would be nonexistent. There have been few true experimental tests of the addition of the resistances principle. The few pertinent packed and plate column studies which have been reported suggest that mass transfer coefficients predicted by the addition of independently measured resistances can be in error by as much as a factor of two (*13*). On the other hand, reasonable agreement has been shown with the addition of the resistances principle in the case of absorption in a stirred flask (*7*). Recently King has analyzed the underlying assumptions of the addition of the resistances principle and has shown that in a number of instances its application can lead to sizable errors (*13*).

The present work had four primary objectives:

1. To develop a simple laboratory device in which convective gas-liquid mass and heat transfer may be investigated under controlled and analyzable conditions in *both* phases.
2. To incorporate in the design facilities for probing local concentrations and temperatures.
3. To ascertain the effect of a tangential velocity at the interface upon interphase mass transfer.
4. To examine situations where the resistance to mass transfer is distributed between phases.

It might also be mentioned that the apparatus had to be sufficiently flexible to accommodate ultimately such studies as simultaneous heat and mass transfer, the initiation of convective cells, and absorption with chemical reaction.

To accomplish these objectives it was essential to select an apparatus which would overcome some or all of the difficulties which have been encountered with other devices. Schemes involving liquid flow over vertical surfaces have been plagued with rippling. To overcome this complication many studies have been made with short exposures. In these cases hydrodynamic end effects become significant. The problems of rippling and end effects may be minimized by the use of a reasonably long horizontal exposure. Problems of thermal insulation of the two contacting phases prior to and during the exposure are particularly acute in many devices. It was also desirable to select an apparatus large enough to allow probing of the phases. Visibility of the contacting phases was another criterion.

EXPERIMENTAL DESIGN

The device which was finally selected is a rectangular channel with high aspect ratio. Figure 1 is a schematic diagram of the entire apparatus. The central portion of the design is a transparent Lexan polycarbonate channel, which consists of a 1.50-ft. long test section between two 2.50-ft. long calming sections. The test section has a cross section 1 in. high and 3 in. wide, with each phase being ½ in. thick. The aspect ratio, the ratio of the channel width to the thickness of one phase, is sufficiently high so that the central inch of the channel width may be assumed to have the fluid mechanics of flow between two flat plates. In this central region the flow velocities vary by no more than 3% in the horizontal direction. The liquid surface velocity employed for the analysis of the data allowed for the drag of the flowing gas phase (*6*) and for the effect of the side walls upon the average velocity in the center section. Tang and Himmelblau (*21*) have solved the momentum equation for laminar two-

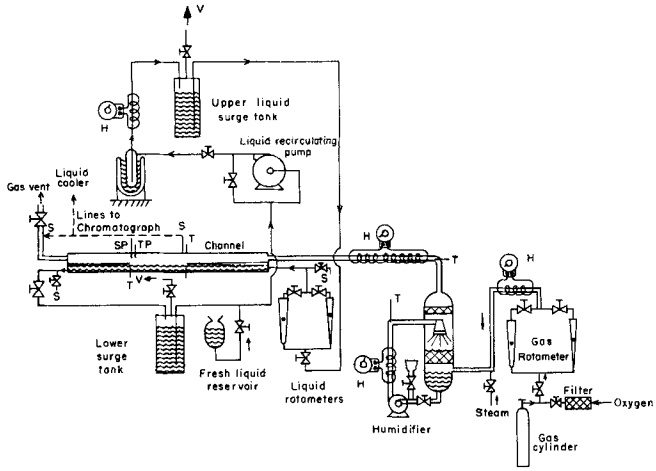

Fig. 1. Schematic diagram of the experimental apparatus. *H*, heater using heating tape and controlled by a Variac. *S*, sample point. *SP*, sample probe used in taking profiles. *T*, temperature measurement point. *TP*, temperature probe designed for taking profiles. *V*, vent on surge tanks.

phase flow in a rectangular duct. A comparison of this solution with the simpler case of two-phase flow between two flat plates for the gases and liquids used in this experimental study indicated that in all cases the average velocity over the whole channel predicted by the latter solution for a given flow rate is 0.915 times the actual average velocity in the center section. This correction factor was used throughout the experimental program.

The gas and liquid leaving the channel were each segregated into three streams by means of vertical divider plates. Only the fluid in the central one inch was used for mass transfer analyses. The two phases are separated by a thin horizontal metal divider in each of the calming sections. Therefore the downstream calming section is divided into a total of six compartments.

Gas, either from the building supply or from cylinders, passes through rotameters before entering the humidifier. In the humidifier the gas is saturated with the nontransferring component of the liquid phase. At the exit of the test section the gas phase vertical concentration profile may be sampled by means of a micrometer type of probing device. This consists of a micrometer barrel, through the center of which passes a stainless steel hypodermic tube with an I.D. of 0.035 in. The end of the tube is bent at right angles to the micrometer so that when the barrel is mounted on the top wall of the channel, the open end of the tube faces into the gas flow. The samples from the probe are piped directly to a gas sample valve on an Aerograph A-90-P2 gas chromatograph. The channel was under a slight positive pressure (always less than 1 lb./sq.in.gauge) to allow sampling. In all cases the rate at which the samples flowed from the sampler to the chromatograph was never greater than the rate of gas impingement at the end of the sample tube. The rate of sample withdrawal was monitored with a rotameter, and was easily set by means of a needle valve. Before the gas is vented to the atmosphere, the cup-mixing concentration is sampled at the exit of the downstream calming section. Here again the samples are piped directly to the chromatograph. The column which was found to be best suited to the analysis of all the systems used was a dual column consisting of 10 ft. of Halomid M-18 and 10 ft. of Ethofat.

Early problems with liquid level control in the channel made conversion from a once-through type system to a recirculating system desirable. A Vanton pump is used to recirculate the liquid. Because of the tendency of the pump to surge slightly, 2-gal. brass surge tanks were placed before and after the pump. One is situated near the ceiling and the other near the floor. Liquid leaving the pump passes through a cooling unit and a heater; it then flows to the ceiling surge tank and moves down to the rotameters and is fed into the lower half of the channel. After it is contacted with the gas, the liquid is drawn from the channel and flows to the lower surge tank. It is then recycled. While cocurrent operation is illustrated in Figure 1, countercurrent contacting may be carried out by simply reversing the liquid piping scheme.

Sampling in the liquid phase is carried out at the inlet and exit of the channel. If the two components of the mixture in question had a sufficient difference in refractive index, a Zeiss differential interferometer was used to analyze the mixture. In the other cases, the liquid sampling facilities of the chromatograph were employed.

Temperatures were measured with copper-constantan thermocouples at some points and by thermistors at others. All places at which measurements are made are indicated by a *T* in Figure 1. A thermal probe, almost identical in design to the micrometer probe used for concentration profiles, is mounted on the test section exit. Temperature profiles could be taken with this probe, whose sensing element is a small, bare thermistor.

The channel was maintained exactly horizontal in all the present work, since the hydraulic gradient along the channel was in all cases negligible. The channel supports are so constructed as to allow operation with the channel inclined to the horizontal, if desired.

A typical experiment would consist of the following steps:

1. A liquid solution was pumped through the system at the desired flow rate and the liquid level in the channel was established at the divider plates. Liquid interfacial velocities ranging from 2.5 to 10 cm./sec. were used in this study. The latter figure corresponds to a Reynolds number of 885, based upon the hydraulic radius, for flowing ethanol.

2. At the start of a series of runs gas samples were taken for a very low main gas stream flow rate. This served to establish the concentration and chromatograph peak area corresponding to saturation of the gas phase with the transferring component of the liquid.

3. A higher gas rate was set and the appropriate concentration profile and cup-mixing concentration samples were analyzed. The gases used included oxygen, carbon dioxide, and helium. Maximum flow rates of about 700 cc./sec. were used; the resulting maximum gas phase Reynolds number was about 1,150 for oxygen.

4. The liquid phase was sampled during the runs and analysis was performed later.

5. Control of the temperatures was accomplished by the heaters and coolers shown in Figure 1. Temperatures were measured at the indicated points.

More details of the construction and operation of this apparatus may be found elsewhere (*4*).

Channels have been used in several earlier gas-liquid mass transfer studies (*8, 9, 12, 20, 22, 23*). Gartside and Goodridge (*8, 9*) measured velocity profiles in a slightly inclined channel and examined the absorption of carbon dioxide into water. Their hydrodynamic results were in basic agreement with those predicted for laminar liquid flow down an inclined plane; while their mass transfer measurements, which were entirely liquid phase controlled, agreed substantially with the Higbie penetration model (*11*). Tang and Himmelblau (*20*) studied liquid phase-controlled gas-liquid mass transfer in stratified, laminar two-phase flow in a horizontal rectangular channel. Pure carbon dioxide was absorbed into water. The absorption rates were found to be predicted satisfactorily by the penetration theory, with an experimental scatter of less than 5%.

On the basis of these two channel experiments as well as most other available liquid phase-controlled mass transfer experiments, it was anticipated that the penetration model would be applicable in the liquid phase in the present series of experiments; therefore no experimental verification of this fact was carried out. The liquid phase never achieved more than 3% equilibration with the bulk gas phase composition.

EXPERIMENTS WITH NO INTERFACE MOTION

The first series of runs involved the evaporation of stagnant ethanol into a flowing gas, and was used as a check upon the hydrodynamics of the gas phase. The channel was half filled with pure ethanol, and this stagnant liquid phase was exposed

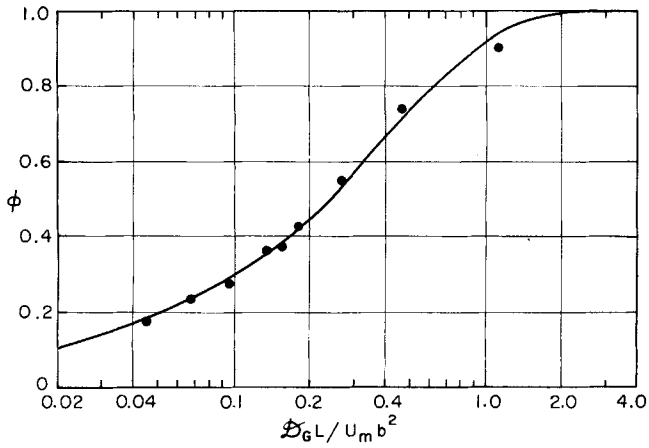

Fig. 2. A comparison of runs with zero interfacial velocity with solution of Butler and Plewes (3). • • • data; ——— theory.

to a series of nine different flow rates of pure nitrogen. This is the experimental situation—a zero interfacial velocity, a parabolic velocity profile, and mass transfer from one side only—for which Butler and Plewes have solved the convective transport equation (3, 6). The interfacial velocity which was caused by drag on the liquid by the gas may be shown to be insignificantly small.

The temperature of the gas-liquid interface was estimated by extrapolation of the measured temperature profile at the test section exit to the interfacial value. The temperature variation across the gas phase was never more than 3°C. The physical properties of the system were estimated at this interfacial temperature (never more than 3° removed from 22°C.). The ethanol concentration in the exit gas was measured and the mean fraction saturation was determined by allowing for the effect of temperature on the chromatograph peak area for total saturation (that is, the variation of ethanol vapor pressure with temperature).

Theory and experiment are compared in Figure 2. The solution of Butler and Plewes for the mean fraction saturation as a function of modified Graetz number ($D_G L/U_m b^2$) is shown as a solid curve. The ordinate may be converted from ϕ to the Stanton number ($k_{cG}\ ave/U_m$) by multiplying ϕ by b/L. The mass transfer coefficient $k_{cG,ave}$ is the average for the exposure based upon the initial driving force. The theoretical curve shown postulates that the ethanol concentration level in the gas at the interface is low enough to have no effect on the mass transfer coefficient. Actually the vapor pressure of ethanol at 22°C. is 48 mm. Hg, and an increase of about 2% in the theoretically predicted ϕ would be expected for this concentration level. The effect would hardly be noticeable. The experimental data agree with theory to better than 5 mole %, which is well within the estimated experimental error.

An experimental concentration profile for a gas flow rate of 203 cc./sec. is compared with the profile predicted by the solution of Butler and Plewes (the solid curve) in Figure 3. Here the agreement is better than 3 mole %, with no readily discernible trend in this error. The cup-mixing concentration based upon an integration of the concentration profile was essentially equal to the theoretically predicted value.

GAS PHASE-CONTROLLED MASS TRANSFER WITH A MOVING INTERFACE

A series of experiments was carried out for the evaporation of pure liquid ethanol flowing in cocurrent motion with the gas phase. Since there was no resistance to mass transfer in the liquid phase, this problem is the one solved in Part I (6) for a single phase with a cocurrent moving interface and parabolic velocity profile. The interface has a constant concentration, different from that in the entering gas stream. The other boundary is a solid wall with zero mass flux. This solution is presented in Figure 8 of reference 6.

Oxygen and carbon dioxide were used. Again the physical properties of the system were estimated at the interfacial temperature, which was never more than 2°C. below the temperature of the two phases. For each gas three different liquid flow rates were used. The range of U_m/U_0 covered was from 0.5 to 12. A concentration profile was obtained for one run for each liquid rate with carbon dioxide. In all, seventy runs were carried out; these are reported in their entirety elsewhere (4).

Figure 4 shows data for various carbon dioxide flow rates with the liquid flowing at 51.0 cc./sec. The mean fraction saturation of the exit stream is shown as a function of the modified Graetz number ($D_G L/U_m b^2$). The solid line shows the computer solution (6) for the experimental conditions allowing for the interfacial velocity, while the dotted line is the solution of Butler and Plewes for no interfacial velocity (3, 6). There is a substantial enhancement of mass transfer due to the interfacial

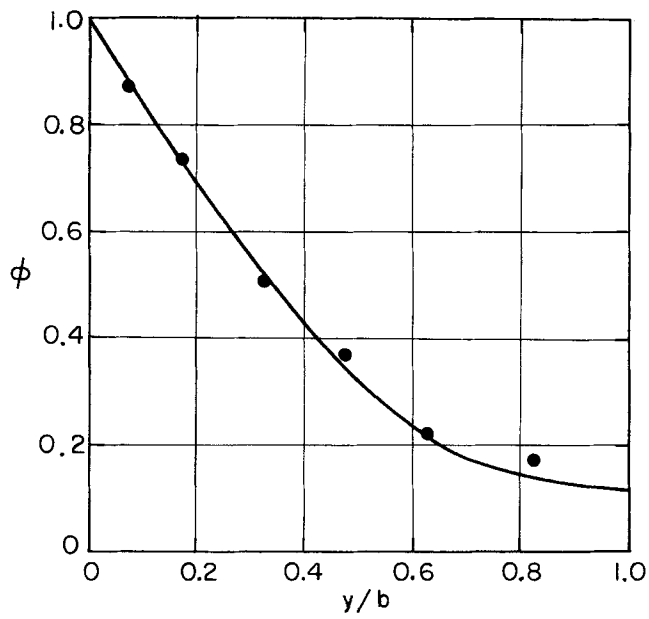

Fig. 3. Concentration profile for run 10. • • • data; ——— theory.

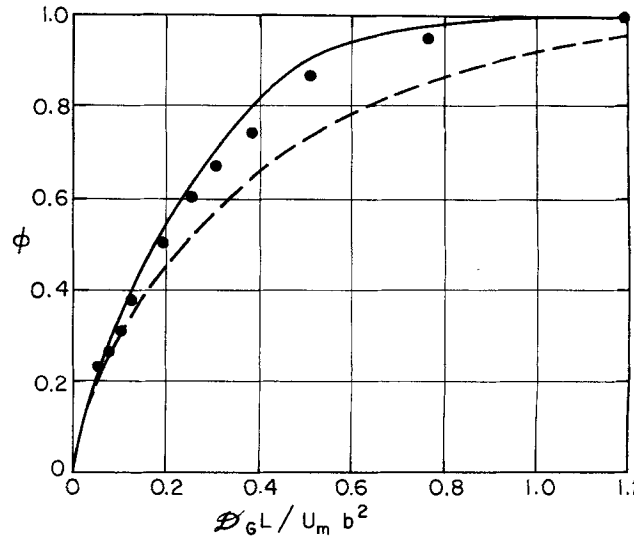

Fig. 4. Mean fraction saturation as a function of the Graetz number for cocurrent motion of carbon dioxide and ethanol (51.0 cc./sec.); • • • data; — — — theory for zero interfacial velocity; ——— computer solution for experimental conditions.

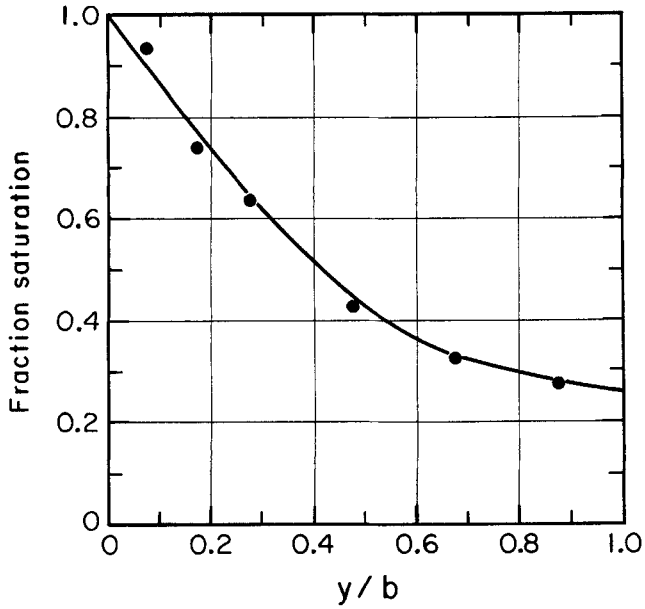

Fig. 5. A typical cocurrent concentration profile. ● experimental data; ——— theory.

velocity. Generally the experimental data are slightly below the theoretical value for a moving interface; however, the data agree within the estimated experimental error of 10%. The concentration profile which was performed in this particular series is shown in Figure 5. The cup-mixing concentration of this run is 50.5% of saturation. In Figure 5 the local fraction saturation is plotted as a function of distance from the interface. The concentration profile generated by the computer solution for the experimental flow conditions (the solid curve) may be compared with the experimental data. The agreement is satisfactory.

The solution for mass transfer to a gas phase with an interfacial velocity U_0 and a constant positive slope a in the velocity profile has been shown to be valid for a parabolic profile up to 50% of saturation (6). The modified version of the Beek and Bakker (2) solution for this case has been discussed previously (6). The local mass transfer coefficient can be integrated as a function of the downstream distance from the start of the exposure to give an average mass transfer coefficient k_c,ave. The uppermost solid line in Figure 6 shows a dimensionless representation of the solution for this average coefficient. All the appropriate data for both oxygen and carbon dioxide runs are also shown as a series of squares. The agreement between the theory and the experimental data is within the estimated error of the method. The good agreement

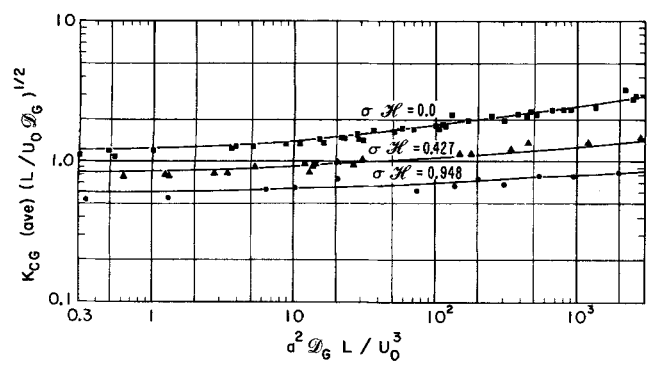

Fig. 6. Cocurrent gas phase-controlled and interphase mass transfer data. ■ gas phase-controlled data; ▲ data for the evaporation of ether into carbon dioxide; ● data for evaporation of ether into helium; ——— theory for the corresponding data.

between theory and data for this situation indicates that hydrodynamic end effects, such as the initial acceleration of the gas and the liquid after the entry divider plate, are not significant. The length of the text section was not altered in the present study, but concentration probes have successfully been made half way along the channel in subsequent work.

COCURRENT INTERPHASE MASS TRANSFER WITH DISTRIBUTED CONTROL

There appears to have been no previous experimental studies of interphase mass transfer with control distributed between the phases carried out under conditions where the behavior could be explicitly predicted using the convective equations of change.

Two series of experiments were carried out in cocurrent flow. In the first carbon dioxide was the gas phase, while in the second the gas was helium. In both cases dilute solutions of reagent grade diethyl ether (about 0.5 mole %) in ethanol were used as the liquid. Both gases were saturated with ethanol in the humidifier so that only ether was evaporated.

Since the diffusion coefficient of ether in ethanol at high dilution had not been reported previously, this quantity was measured by a diaphragm cell technique, which has been reported elsewhere (5). The result is 0.871×10^{-5} sq.cm./sec. $\pm$ 5.0%. Other physical properties employed to analyze the data are tabulated elsewhere (4).

It has been shown in Part I (6) that for interphase mass transfer the factor $(D_G/D_L)^{1/2}(H/RT)$ determines the degree to which the gas phase or the liquid phase controls the mass transfer process. This constant is equal to 0.427 for the runs with carbon dioxide and 0.948 for the runs with helium. Thus the control was at about 80% in gas phase in the former case, and 50% in the gas in the latter. Because of the low concentration of ether the maximum drop in the interfacial temperature was less than 0.1°C. Hence this factor was not a consideration in these runs.

Each series of runs was carried out with the use of four different liquid flows and several different gas flow rates. Forty-four runs was made in all. It was found that if the gas rate was above about 200 cc./sec. somewhat greater mass transfer coefficients were observed than could be explained by laminar theory. Since this was not observed in the analysis of the single phase case, it appears likely that some rippling of the liquid interface was being induced.

The results of all the runs which have sufficiently high flow rates to prevent the analytic model for a linear velocity profile in the gas from being unrealistic (usually above 60 cc./sec.) are shown in Figure 6. Following the model, we give the results as a plot of $K_c,ave(L/U_0D_G)^{1/2}$ as a function of the group a^2D_GL/U_0^3 for different values of the parameter $(D_G/D_L)^{1/2}H$. The line which shows complete control of the gas phase and the corresponding data are given for comparison. The triangles give the values for carbon dioxide, while the circles are the points for helium. The theoretical curves are shown to agree with the data within the limits of the accuracy of this series of experiments. Because of the added difficulty of running an interphase experiment, it is estimated that the experimental error was about 15%. Six spurious data points have been omitted from Figure 6 for the sake of clarity; they do not alter conclusions to be drawn from that figure.

The data could also be compared with the exact computer solution for mass transfer between two cocurrent phases with parabolic velocity profiles (6). Some typical results are shown in Figure 7. The mass transfer coefficient is the average overall coefficient based on a con-

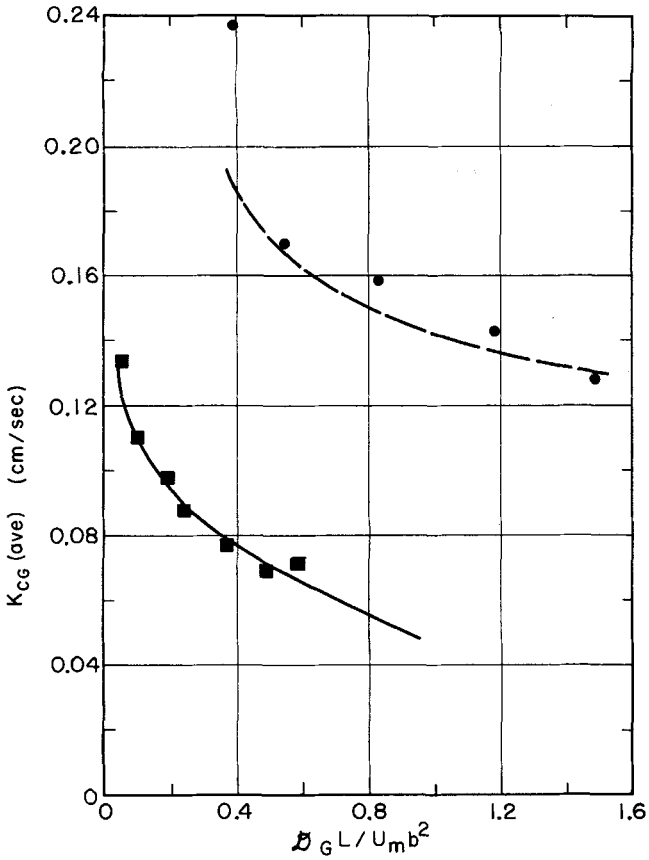

Fig. 7. Interphase mass transfer and a comparison with an exact computer solution. ■ carbon dioxide data; ——— carbon dioxide theory; ● helium data; — — — helium theory.

centration driving force in gas phase units and is expressed in centimeters per second. Two series of runs are shown, both at a liquid rate of 30.86 cc./sec. The squares represent the data for mass transfer into carbon dioxide, while the circles represent the helium results. The two lines are the theoretical curves for the experimental flow rates. Within the experimental error of the method, data followed theory in all but a few cases. We may conclude therefore that a valid model has been developed to predict interphase mass transfer coefficients in laminar cocurrent flow.

MASS TRANSFER IN COUNTERCURRENT FLOW

In all the previous cases cocurrent flow was investigated. However countercurrent flow is of much more importance industrially. It is normal design practice to assume that a mass transfer coefficient for countercurrent operation is the same as that for cocurrent flow, and that there is an increased driving force. The question of the effect of interfacial velocity upon mass transfer coefficients again casts some doubt upon this procedure.

In channel flow both phases are confined and in countercurrent flow there must be a point of zero velocity at some level. Because the liquid is more viscous than the gas, the point of zero velocity will usually lie within the gas phase. Hence there will be an area in the gas phase near the interface where the flow is in the same direction as the liquid interface, while the main bulk of the gas phase is flowing in the opposite direction. Since only molecular diffusion may take place at the point of zero velocity, it might be anticipated that the mass transfer coefficient would be less than would be predicted by the corresponding cocurrent theory. This conclusion was derived theoretically for very short exposures in Part I (*6*).

The runs for the evaporation of ethanol and pure carbon dioxide were repeated, but this time the two fluids flowed in opposite directions. No particular problem due to ripples or level control was encountered in operating countercurrently. Thirty-three runs were carried out at three different liquid rates.

The results for the highest liquid rate, 53.7 cc./sec., are shown in Figure 8. The average mass transfer coefficient based on the driving force between the entering phases is plotted as a function of the modified Graetz number. The dotted line is the solution of Butler and Plewes for no interfacial motion (*3, 6*). It is evident that the flow reversal does decrease the mass transfer coefficient to a considerable extent.

With the data for countercurrent flow available, it became desirable to develop some theoretical interpretation of the experiments. The existence of a flow reversal makes an exact solution to this problem much more difficult. The problem lies in the fact that the part of the gas which flows in the same direction as the liquid enters the test section at the downstream end of the exposure with a definite but unknown concentration. Any numerical solution of this problem would necessarily be an iterative one. A simpler approximation was made in this case in lieu of a more elaborate solution. Since the backflow enters at a concentration which is close to equilibration, it is assumed that, as a limiting case, the area between the interface and the flow reversal is a stagnant film. The Graetz model is assumed to hold in the remainder of the channel. If it is assumed that the resistances to mass transfer may be added independently, the result is

$$\frac{1}{k_{cG}(ave)} = \frac{1}{k_{c,Gz}(ave)} + \frac{1}{k_{c,film}(ave)} \qquad (1)$$

where

$$k_{c,film}(ave) = D_G/\Delta \qquad (2)$$

and

$$k_{c,Gz}(ave) = f\left(\frac{D_G L}{U_m (b-\Delta)^2}\right) \qquad (3)$$

The variable Δ is the distance between the interface and

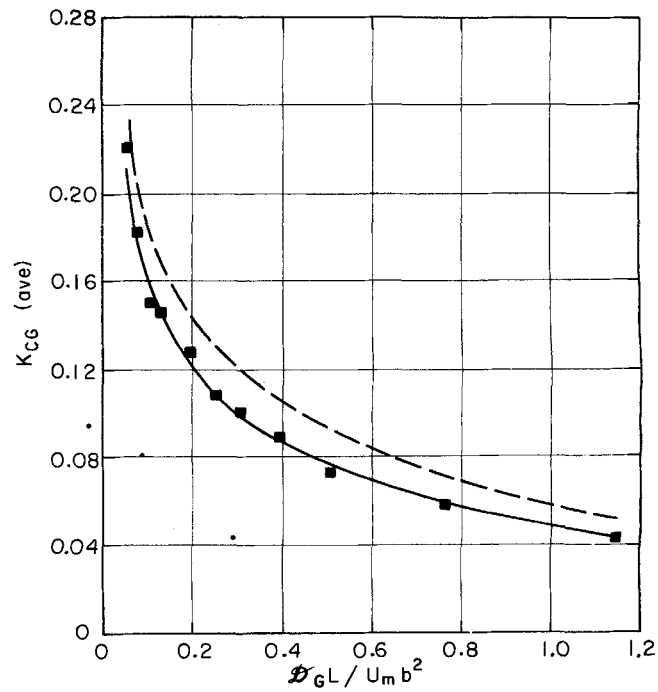

Fig. 8. Countercurrent mass transfer of ethanol into carbon dioxide with ethanol flow rate = 53.70 cc./sec. ■ data; ——— countercurrent theory; — — — Graetz solution (zero interfacial velocity).

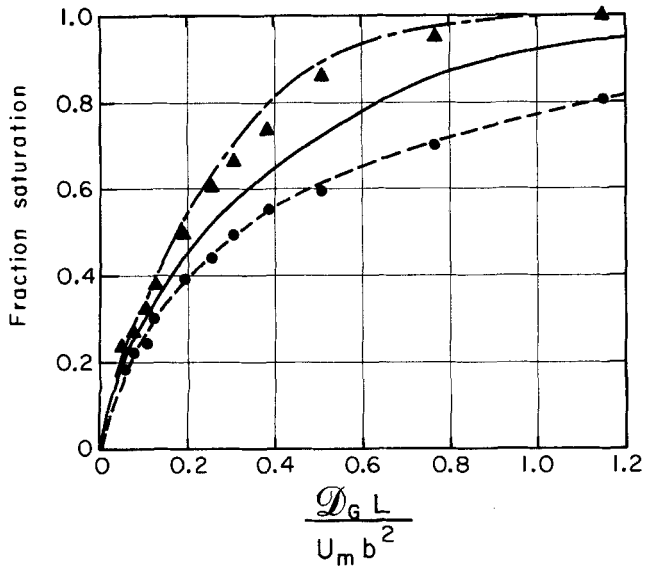

Fig. 9. A comparison of laminar, single cocurrent and countercurrent data. ▲ cocurrent data; —— — —— cocurrent theory; ——— Graetz solution; ● countercurrent data; — — — countercurrent theory.

the flow reversal. The point of flow reversal may be found from the following equation:

$$\Delta/b = \frac{U_0}{3U_0 + 6U_{Gm}} \tag{4}$$

where positive values are used for both velocities. Equation (4) may be obtained from Equations (2) and (4) of Part I. The average velocity used in the Graetz portion of the solution is based on the flow of the inlet gas plus the backflow (usually a small quantity), averaged over the width $b - \Delta$.

In Figure 8 the solid line represents the prediction of this simplified theory for the experimental liquid rate and the range of gas rates used. The flow reversal zone in the gas varied from 0.009 to 0.29 cm. in thickness. The data agree almost quantitatively with the proposed theory, certainly within the error of the experimental method.

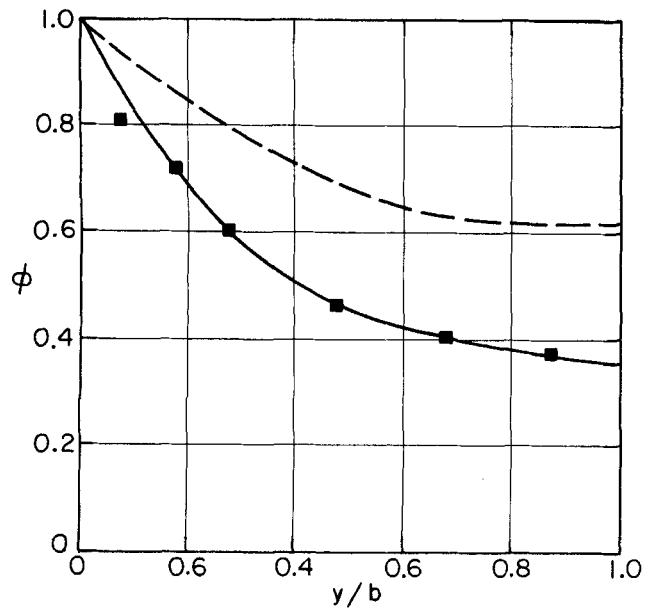

Fig. 10. Concentration profile for mass transfer in countercurrent flow. ■ data; ——— best fit of data; — — — theoretical concentration profile for the corresponding cocurrent conditions.

For the highest liquid flow rate a comparison is made of the cocurrent data with the countercurrent data in Figure 9. The solution for zero surface motion is included for comparison. Again the ordinate may be converted from φ to the Stanton number based on the initial driving force by multiplying by the factor b/L. It is quite evident that the direction of motion of the interface is important and that one must exercise great care in applying cocurrent data to countercurrent design.

Three concentration profiles were carried out for the evaporation of ethanol into carbon dioxide with countercurrent operation. One of these is represented in Figure 10. The best line is drawn through the data, and the profile is compared with that which is expected for the corresponding cocurrent case. The difference is quite sizable. The other two profiles are reported elsewhere (*4*).

Countercurrent experiments with the mass transfer resistance distributed between phases were performed with the same systems as were used in the cocurrent studies. The emphasis was laid on helium data because of the fact that control was more evenly divided between the phases in this case. The results for a series of helium runs with a liquid rate of 61.82 cc./sec. as well as a series for carbon dioxide with a liquid rate of 30.86 cc./sec. are shown in Figure 11. The computer solutions for the corresponding cocurrent interphase mass transfer cases are shown as dotted lines in each case. Here again some theoretical analysis of the countercurrent situation was necessary.

If we are considering interphase mass transfer in the flow between two flat plates, the resistance of the liquid phase must be added to the two assumed for the gas phase alone in Equation (1). The resulting equation is

$$\frac{1}{K_{cG}(ave)} = \frac{1}{k_{cG}(ave)} + \frac{\mathcal{H}}{k_{cL}(ave)} \tag{5}$$

where the individual gas phase resistances are defined in Equations (2) and (3) and the liquid phase mass transfer coefficient is defined as

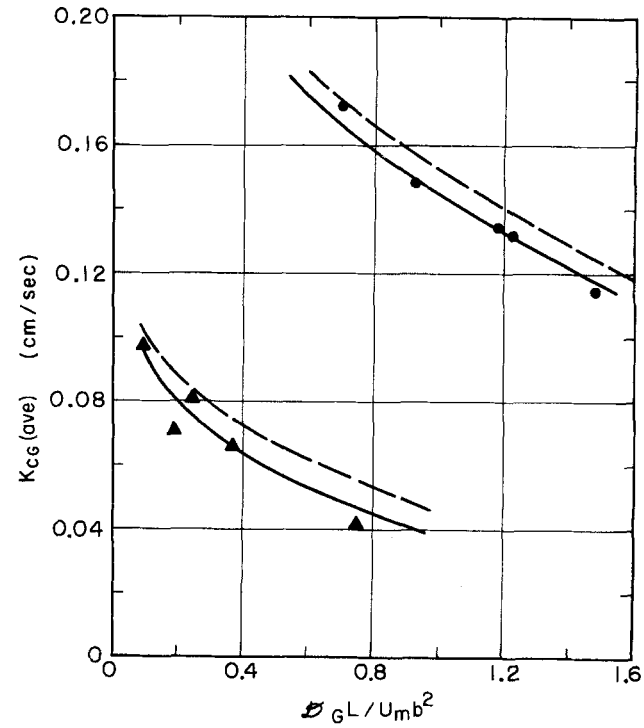

Fig. 11. Interphase countercurrent mass transfer data and theory. ▲ carbon dioxide data; ● helium data; ——— countercurrent theory; — — — theory with no flow reversal.

$$k_{cL}(ave) = 2\left(\frac{D_L U_0}{\pi L}\right)^{1/2} \qquad (6)$$

The fact that the counterflow models chosen by King (*14*) showed an appreciable deviation from additivity suggests that this model might predict mass transfer coefficients which are slightly higher than one would actually measure. The predictions of this theory for the experimental flow conditions are shown as the solid curves in Figure 11. It is evident that the helium data, shown by circles, follow the predictions of the simple model for interphase mass transfer in countercurrent flow. The carbon dioxide data are more scattered and the agreement with the theory is not as good as in the helium runs. Problems with the operation of the chromatograph in the carbon dioxide runs are the probable cause of the scatter. It may be stated, primarily on the basis of the helium runs reported here and elsewhere (*4*), that the simple countercurrent theory stated in Equation (5) adequately describes the results. The reversal in the gas phase velocity reduces the mass transfer coefficient in these cases.

SURFACTANT ACCUMULATION

A series of experiments was carried out in which diethyl ether was evaporated from a 0.5 mole % solution in water with cocurrent flow. Three gases—oxygen, carbon dioxide, and helium—were contacted with the ether-water solutions.

To analyze the data it was necessary to obtain a diffusion coefficient for the ether-water solutions at high dilution. This measurement was carried out by the same diaphragm cell technique used for the ether-ethanol system. At 25°C. the measured result was

$$D_{\text{ether}-H_2O} = 0.962 \times 10^{-5} \text{ sq.cm./sec.} \pm 3.5\%$$

Rossi et al. (*17*) have reported a value of 0.878×10^{-5} sq.cm./sec. for the same system at 20°C. Therefore, if $D\mu/T$ is assumed to be a constant, the two values agree to within 2%.

When the runs for evaporation of ether from water solution were analyzed and compared with the interphase mass transfer theory described in Part I (*6*), it was found that the mass transfer coefficients were lower than the predicted values by at least a factor of two. Merson and Quinn (*16*) have shown that trace contaminants in distilled water can form a film of surfactants which tends to cover horizontal surfaces completely. This is accompanied by a tendency to stagnate the interface. Visual observation of the surface motion with gas bubbles, inserted for that purpose, confirmed that the velocity of the interface was very much slower than that expected for the hydrodynamic conditions prevalent in the channel. The circulation pattern reported by Merson and Quinn, forward motion in the central region and backflow near the walls, was also observed in his study. The experimental mass transfer coefficients indicate that the interfacial velocity in the center of the channel was about 10 to 20% of the predicted velocity, if a linear velocity gradient model is applied to both phases. This was confirmed by the visual observations mentioned above.

Ethanol interfaces showed no tendency to stagnate, again as confirmed by visual observations of bubble motion. This may result from the fact that the surface tension of ethanol is so much lower than that of water and from the fact that ethanol is more of an amphiphilic molecule. Acrivos and Kashiwagi (*1*) have found that the backflow at the edges of a nearly horizontal flow of liquid over a surface only occurs for materials with high interfacial tensions. Subsequent experiments have involved the flow of a C_{12}-C_{14} paraffin hydrocarbon liquid in the channel. Measured surface velocities again agree with the theoretical for no surface stagnation.

CONCLUSIONS

The conclusions drawn from this experimental study may be summarized as follows:

1. A horizontal rectangular channel may be used to study laminar interphase mass transfer under controlled hydrodynamic conditions in both phases.
2. When there is no interfacial motion, mass transfer to the gas phase of the channel may be predicted by the solution of Butler and Plewes (*3*). This was confirmed for the evaporation of ethanol into various gases.
3. Cocurrent motion of the interface enhances mass transfer to the extent predicted by the theoretical portion of this study (*6*). The modified solution of Beek and Bakker (*2, 6*) is also valid for the appropriate experimental data.
4. Countercurrent motion of the interface decreases gas phase mass transfer coefficients. A simple model developed in this study quantitatively correlated the experimental data.

ACKNOWLEDGMENT

This work was performed in the Lawrence Radiation Laboratory under the auspices of the U.S. Atomic Energy Commission.

NOTATION

- a = slope of the gas phase velocity at the interface, sec.$^{-1}$
- b = thickness of the gas phase, cm.
- D = diffusion coefficient, sq.cm./sec.
- Gz = modified Graetz number, $D_G L/U_m b^2$
- H = Henry's law constant, (atm.)(cc.)/g.-mole
- $\mathcal{H}$ = dimensionless Henry's law constant (H/RT)
- K_c = local overall mass transfer coefficient based on the initial driving force, cm./sec.
- $K_c(ave)$ = average overall mass transfer coefficient based on the initial driving force, cm./sec.
- k_c = local individual phase mass transfer coefficient based on the initial driving force, cm./sec.
- $k_c(ave)$ = average individual phase mass transfer coefficient based on the initial driving force, cm./sec.
- L = length of the exposure, cm.
- R = universal gas constant, (atm.)(cc.)/(g.-mole)(°K.)
- T = absolute temperature, °K.
- U = velocity of the flowing phases, cm./sec.
- U_0 = interfacial velocity, cm./sec.
- y = coordinate direction perpendicular to the interface, cm.
- Δ = distance between the interface and the flow reversal in countercurrent flow, cm.
- μ = liquid viscosity
- φ = mean fraction saturation; that is, increase in solute concentration plus increase for thermodynamic equilibrium

Subscripts

- film = estimated by film model
- G = gas phase
- Gz = estimated by the Graetz solution
- L = liquid phase
- m = average in the gas phase

LITERATURE CITED

1. Acrivos, Andreas, and B. R. Kashiwagi, paper submitted to *Ind. Eng. Chem.* (1966). Research Results Service MS-65-505.

2. Beek, W. J., and C. A. P. Bakker, *Appl. Sci. Res.*, **A10**, 241 (1961).
3. Butler, R. M., and A. C. Plewes, *Chem. Eng. Progr. Symp. Ser. No. 10*, **50**, 121 (1954).
4. Byers, C. H., and C. J. King, *U.S. Atomic Energy Comm. Rept. UCRL-16535* (1966).
5. ———, *J. Phys. Chem.*, **70**, 2499 (1966).
6. ———, *AIChE J.*, **13**, 628-636 (1967).
7. Goodgame, T. H., and T. K. Sherwood, *Chem. Eng. Sci.*, **3**, 37 (1954).
8. Goodridge, Francis, and G. Gartside, *Trans. Inst. Chem. Engrs.*, **43**, T62 (1965).
9. *Ibid.*, T74.
10. Hatch, T. F., and R. L. Pigford, *Ind. Eng. Chem. Fundamentals*, **1**, 209 (1962).
11. Higbie, Ralph, *Trans. Am. Inst. Chem. Engrs.*, **31**, 365 (1935).
12. Jaymond, M., *Chem. Eng. Sci.*, **14**, 126 (1961).
13. King, C. J., *AIChE J.*, **10**, 671 (1964).
14. ———, *Ind. Eng. Chem. Fundamentals*, **4**, 125 (1965).
15. Lewis, W. K., *Mech. Eng.*, **44**, 445 (1922).
16. Merson, R. L., and J. A. Quinn, *AIChE J.*, **11**, 391 (1965).
17. Rossi, C., E. Bianci, and A. Rossi, *J. Chim. Phys.*, **55**, 99 (1958).
18. Scriven, L. E., and R. L. Pigford, *AIChE J.*, **4**, 439 (1958).
19. *Ibid.*, **5**, 397 (1959).
20. Tang, Y. P., and D. M. Himmelblau, *ibid.*, **9**, 630 (1963).
21. ———, *Chem. Eng. Sci.*, **18**, 143 (1963).
22. van Krevelen, D. W., and P. J. Hoftijzer, *Rec. Trav. Chim.*, **68**, 221 (1949).
23. Westkeamper, L. E., and R. R. White, *AIChE J.*, **3**, 69 (1957).
24. Whitman, W. G., *Chem. Met. Eng.*, **29**, 146 (1923).

Manuscript received July 13, 1966; revision received October 13, 1966; paper accepted October 14, 1966. Paper presented at AIChE Detroit meeting.

The Streaming Potential Fluctuations in a Turbulent Pipe Flow

HENRY LIU

University of Missouri, Columbia, Missouri

Accompanied by a brief theoretical consideration, the results of an experimental study of the streaming potential fluctuations in turbulent pipe flows of distilled water are presented. The dependence of the streaming potential fluctuations on turbulent velocity fluctuations and other parameters as indicated by the theory is determined from the experimental data. Information on the characteristics of turbulent velocity fluctuations in the viscous sublayer near a pipe wall have been inferred from the data.

It is well known that surface preferential adsorption of ions causes an electric double layer to exist at any solid-liquid interface (*1* to *4*). For water and solutions thereof, the diffuse layer, which is the outer part of the double layer, extends a distance of the order of 100 Å. or less from the wall (the distance depends on the concentration and valence of the ions in the solution, the dielectric constant, and the temperature of the fluid). When the liquid is forced to flow through a capillary tube, the transport of the diffuse-layer charge by the flow creates a convective electric current in the flow direction. A conduction current of opposite direction develops and a potential difference ψ_s (the streaming potential) arises along the tube. The equation of the streaming potential for a steady laminar flow, as derived by Helmholtz (*5*) and Smoluchowski (*6*), is

$$\psi_s = \frac{\epsilon_0 \kappa \zeta \Delta p}{\mu \sigma_0}$$

Note that the equation is given here in its mks unit form.

In 1928 Reichardt (*7*) showed experimentally that this equation is also valid for turbulent flow, provided that ΔP and ψ_s represent, respectively, the time averages of the pressure and potential differences along the tube. He also predicted that a fluctuating component of the streaming potential would exist in a turbulent flow, although his instrument was not sensitive enough to detect it. Bocquet (*8*) actually measured such a fluctuation in a pipe. He also proposed the idea of utilizing the phenomenon to study turbulence near a wall. Boumans (*9*), Gavis and Koszman (*10* to *13*), and many others have studied electrokinetic phenomena in turbulent flow of low conductivity fluids, with major interests in the mean rather than the fluctuating quantities of the electrokinetic flow. A series of studies of the electrokinetic potential fluctuations in water has been made by Binder (*14*), Chuang (*15*), Duckstein (*16*), and Liu (*17*).

The purpose of this paper is to describe the theory